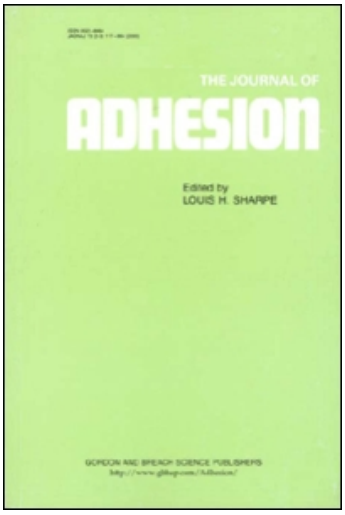

The Journal of Adhesion
Publication details, including instructions for authors and subscription information:
http://www.informaworld.com/smpp/title~content=t713453635

Hygrothermal Properties of Highly Toughened Epoxy Adhesives

A. Ameli[a]; N. V. Datla[a]; M. Papini[b]; J. K. Spelt[a]
[a] Department of Mechanical and Industrial Engineering, University of Toronto, Toronto, Ontario, Canada [b] Department of Mechanical and Industrial Engineering, Ryerson University, Toronto, Ontario, Canada

Online publication date: 10 August 2010

To cite this Article Ameli, A. , Datla, N. V. , Papini, M. and Spelt, J. K.(2010) 'Hygrothermal Properties of Highly Toughened Epoxy Adhesives', The Journal of Adhesion, 86: 7, 698 — 725
To link to this Article: DOI: 10.1080/00218464.2010.482405
URL: http://dx.doi.org/10.1080/00218464.2010.482405

The Journal of Adhesion, 86:698–725, 2010

ISSN: 0021-8464 print/1545-5823 online
DOI: 10.1080/00218464.2010.482405

Taylor & Francis
Taylor & Francis Group

Hygrothermal Properties of Highly Toughened Epoxy Adhesives

A. Ameli[1], N. V. Datla[1], M. Papini[2], and J. K. Spelt[1]
[1]Department of Mechanical and Industrial Engineering, University of Toronto, Toronto, Ontario, Canada
[2]Department of Mechanical and Industrial Engineering, Ryerson University, Toronto, Ontario, Canada

The absorption and desorption of water in two different rubber-toughened epoxy adhesives was measured gravimetrically over a relatively wide range of temperature and relative humidity (RH). The data were fitted to a new diffusion model in which Fick's law was assumed to act in two sequential stages, each with its own diffusion coefficient and saturated water concentration. This "sequential dual Fickian" (SDF) model and a Langmuir-type diffusion model were both able to model the absorption behaviour. The dependence of the five SDF model parameters on temperature and RH was investigated in detail. The two diffusion coefficients were found to be largely independent of RH, while the fractional mass uptake values for each stage increased with RH. The absorption temperature only had a significant effect on the diffusion coefficient of the first stage and the fractional mass uptake of the second stage. Water desorption from the two epoxies was modeled accurately using Fick's law. A significant difference was observed between the amounts of retained water in the two adhesives after drying. The results can be used to predict the water concentration distribution in adhesive joints exposed to environments of changing temperature and RH.

Keywords: Absorption; Desorption; Diffusion; Dual Fickian; Epoxy adhesive; Hygrothermal; Toughened

1. INTRODUCTION

It is widely known that the water ingress plays a significant role in the progressive degradation of the mechanical properties and, hence, the

Received 16 October 2009; in final form 30 January 2010.
One of a Collection of papers honoring David A. Dillard, the recepient in February 2010 of *The Adhesion Society Award for Excellence in Adhesion Science, Sponsored by 3 M*.
Address correspondence to J. K. Spelt, Department of Mechanical and Industrial Engineering, University of Toronto, 5 King's College Road, Toronto, Ontario, Canada M5S 3G8. E-mail: spelt@mie.utoronto.ca

durability of epoxy adhesives. Many of the diffusion models that have been proposed to explain hygrothermal effects in epoxies fall into two categories. One is defined by the assumption that water diffuses into the epoxy and resides in the free volume of the material. The other assumes that absorbed water molecules couple strongly with certain hydrophilic functional groups such as hydroxyls in the epoxy resin. However, some researchers have shown that both physical and chemical mechanisms may occur simultaneously [1–4].

The simplest diffusion model is Fick's law, which assumes that there are no interactions between the absorbed water molecules and the polymer chains. Simple Fickian behavior is observed in epoxies well above the glass transition temperature, T_g [5]. In many cases, however, the simple Fickian model does not represent the absorption process and tends to overestimate water concentration [1–3,6–9]. Such cases are called non-Fickian or anomalous.

One class of diffusion models proposed for the anomalous behaviour of water diffusion into epoxy adhesives is based on modifications to Fick's law. For example, the dual Fickian diffusion model assumes that the diffusion is Fickian, but occurs through two different mechanisms acting in parallel with different diffusion properties [8–10]. The dual Fickian model is, hence, the superposition of two single Fickian models. Fick's law has also been generalized by introducing time-varying diffusion coefficients [1,7] or time-varying boundary conditions [1,2]. In these models, the diffusion coefficient or boundary condition is assumed to take the form of a Prony series which requires finding multiple coefficients and corresponding retardation times. These models introduce many degrees of freedom to the problem and the solution can be cumbersome and time-consuming.

Another class of anomalous diffusion models is based on a combination of physical diffusion and chemical interactions. Several studies, partially reviewed in [11], have been made to clarify the formation and existence of two different states of water molecules in epoxy, termed free and bound. Carter and Kibler [12] suggested a Langmuir-type two-phase diffusion model which assumes the existence of diffusing molecules in free and bound states. The Langmuir model has been used with some success at times [1,6,12].

Unlike absorption, water desorption behavior is normally Fickian [8]. The absorbed water in an epoxy cannot be completely removed in some cases and the existence of retained water after drying at temperatures below T_g has been reported in the literature [13–16]. For example, Moy and Karasz [16] investigated epoxy–water interaction by differential scanning calorimetry (DSC), infrared spectroscopy (IR), nuclear magnetic resonance spectroscopy (NMR), and water absorption/desorption

gravimetric experiments using a tetraglycidyl 4,4-diaminodiphenyl methane/diaminodiphenylsulphone (TGDDM/DDS) resin system. They observed a strong hysteresis related to the desorption process indicating retained amounts of water that could only be removed by heating the epoxy to temperatures above 100°C. Zhou and Lucas [14] showed that retained water after low-temperature desorption was related to the amount of water molecules forming stronger bonds (*i.e.*, multiple hydrogen bonds) with the epoxy network.

The absorption and desorption of water in two different rubber-toughened epoxy adhesives is measured gravimetrically over a relatively wide range of temperature and RH. The data are fitted to a new diffusion model in which Fick's law was assumed to act in two sequential stages, each with its own diffusion coefficient and saturated water concentration. This "sequential dual Fickian" (SDF) model and a Langmuir-type diffusion model are both able to model the absorption behaviour. The dependence of the five SDF model parameters on temperature and RH is investigated in detail. The two adhesives were selected to establish the generality of the SDF model and because they demonstrated different fracture durability behavior in a separate test program.

2. MATHEMATICS OF DIFFUSION MODELS

In this study, a newly developed type of dual Fickian model and a Langmuir-type model were used to characterize the anomalous behaviour of water absorption in two rubber-toughened epoxy adhesives, while a simple Fickian model was employed for the desorption modeling. Based on the size and shape of the wafer samples and the experimental setup, the diffusion was considered as one-dimensional. The initial condition of absorption for both models was assumed to be zero water concentration and the constant saturation concentration value was taken as the boundary condition.

2.1. Dual Fickian Model

In simple Fickian diffusion, it is assumed that the moisture flux is directly proportional to the concentration gradient in a material. The one-dimensional differential equation of Fickian diffusion, the boundary conditions, and the initial condition for absorption to a plane sheet of thickness $2h$ are given as follows:

$$\begin{cases} \frac{\partial C(x,t)}{\partial t} = D\frac{\partial^2 C(x,t)}{\partial x^2} \\ C(x = \pm h,\, t) = C_\infty, \\ C(x,\, t \le 0) = 0 \end{cases} \tag{1}$$

where $C(x, t)$ is the water concentration (% by mass) at any spatial coordinate x (m) and time interval t (s), C_∞ (%) is the saturated moisture concentration, and D (m^2/s) is the diffusion coefficient. The solution to the partial differential equation in Eq. (1) is given by:

$$\frac{C(x,t)}{C_\infty} = 1 - \frac{4}{\pi}\sum_{n=0}^{\infty}\frac{(-1)^n}{2n+1}\exp\left(\frac{-D(2n+1)^2\pi^2 t}{4h^2}\right)\cos\frac{(2n+1)\pi x}{2h}. \quad (2)$$

The fractional mass uptake, M_t (*i.e.*, the total mass uptake of water at time t expressed as a percentage of the initial mass of the sample), can be obtained by integrating Eq. (2) over the spatial variable x:

$$\frac{M_t}{M_\infty} = 1 - \frac{8}{\pi^2}\sum_{n=0}^{\infty}\frac{1}{(2n+1)^2}\exp\left(\frac{-D(2n+1)^2\pi^2 t}{4h^2}\right), \quad (3)$$

where M_∞ is the saturated fractional mass uptake, *i.e.*, the mass uptake at saturation expressed as a percentage of the initial mass of the sample.

In the dual Fickian models present in the literature [8,9,17], two diffusion mechanisms are considered to be working in parallel such that the fractional mass uptake increases continuously until it reaches M_∞. These models are called "parallel dual Fickian" (PDF). The Langmuir-type model and the gravimetric results in this study, however, indicated that there was a pseudo-equilibrium state at intermediate exposure times before reaching the final saturation (Section 4). This has been modeled in the present work by assuming that the pseudo-equilibrium corresponds to the completion of the first uptake mechanism and the start of the second one. Based on this assumption, a new "sequential dual Fickian" (SDF) model was developed in which the moisture concentration at any t and x is determined by:

$$\begin{aligned} C(x,t) = {} & \left(1 - \frac{4}{\pi}\sum_{n=0}^{\infty}\frac{(-1)^n}{2n+1}\exp\left(\frac{-D_1(2n+1)^2\pi^2 t}{4h^2}\right)\right. \\ & \left.\times\cos\frac{(2n+1)\pi x}{2h}\right)\times C_{1\infty} + \phi\,(t - t_d)\times\left(1 - \frac{4}{\pi}\sum_{n=0}^{\infty}\frac{(-1)^n}{2n+1}\right. \\ & \left.\times\exp\left(\frac{-D_2(2n+1)^2\pi^2(t-t_d)}{4h^2}\right)\cos\frac{(2n+1)\pi x}{2h}\right)\times C_{2\infty}, \end{aligned} \quad (4)$$

where $C_{1\infty}$ and $C_{2\infty}$ are the saturated concentrations of the first and second diffusion mechanisms such that $C_{1\infty} + C_{2\infty} = C_\infty$, where C_∞

is the total saturation concentration. D_1 and D_2 are the diffusion coefficients of the first and second moisture uptake mechanisms, respectively. t_d is the time at which the transition from the first diffusion mechanism to the second one occurs, and $\varphi(t)$ is the Heaviside step function defined as:

$$\varphi(t-t_d)=\begin{cases}0, & t<t_d\\ 1, & t\geq t_d\end{cases}. \tag{5}$$

The Heaviside step function in the second part of the right hand side of Eq. (4) ensures that the moisture concentration corresponding to the second mechanism is zero as long as the exposure time is less than t_d. By integrating Eq. (4) over the spatial variable, the fractional mass uptake, M_t, for the SDF model at any time, t, is given by:

$$M_t=\left(1-\frac{8}{\pi^2}\sum_{n=0}^{\infty}\frac{1}{(2n+1)^2}\exp\left(\frac{-D_1(2n+1)^2\pi^2 t}{4h^2}\right)\right)\times M_{1\infty}+\phi(t-t_d)$$
$$\times\left(1-\frac{8}{\pi^2}\sum_{n=0}^{\infty}\frac{1}{(2n+1)^2}\exp\left(\frac{-D_2(2n+1)^2\pi^2(t-t_d)}{4h^2}\right)\right)\times M_{2\infty}, \tag{6}$$

where $M_{1\infty}$ and $M_{2\infty}$ correspond to the first and second uptakes, respectively, and $M_{1\infty}+M_{2\infty}=M_\infty$ (Fig. 1). The fractional mass

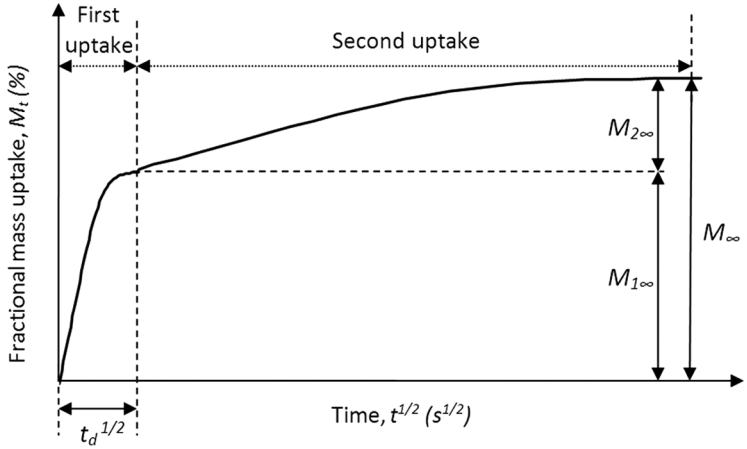

FIGURE 1 Schematic illustration of the sequential dual Fickian (SDF) model.

uptake at any time t, M_t was determined experimentally using gravimetric measurements and its value is given by:

$$M_t = \frac{W_t - W_i}{W_i} \times 100\%, \tag{7}$$

where W_i and W_t are the sample weights before any exposure and after an exposure time of t, respectively. Thus, the model has 5 parameters: D_1, D_2, $C_{1\infty}$, $C_{2\infty}$, and t_d. The present data were used to identify the dependence of these parameters on temperature, T, and relative humidity, RH, in order to make the model predictive for a range of environmental conditions.

2.2. Langmuir Model

Carter and Kibler proposed a Langmuir-type adsorption theory to model the anomalous behaviour of moisture diffusion in polymers [12]. This model assumes the existence of diffusing molecules in mobile and bound states, each with probabilities of interchanging their states. Based on this model, for the one-dimensional case, the molecular number densities at exposure time, t, and spatial coordinate, x, satisfy the coupled pair of equations:

$$D_L \frac{\partial^2 n_m}{\partial x^2} = \frac{\partial n_m}{\partial t} + \frac{\partial n_b}{\partial t} \tag{8}$$

$$\frac{\partial n_b}{\partial t} = \gamma n_m - \beta n_b, \tag{9}$$

where D_L is the diffusion coefficient and n_m and n_b represent the number of mobile and bound water molecules per unit volume. γ and β are the probabilities per unit time (s^{-1}) that mobile and bound molecules will change their respective states. Solving these equations with the equivalent initial and boundary conditions as for the SDF model gives the number of molecules at time t and position x. The total number of water molecules per unit volume in an adhesive at time t, N_t, is approximated by [6]:

$$\text{for short exposure times: } \frac{N_t}{N_\infty} \cong \frac{4}{\pi^{3/2}} \left(\frac{\beta}{\beta + \gamma} \right) \sqrt{\kappa t} \tag{10}$$

$$\text{for long exposure times: } \frac{N_t}{N_\infty} \cong 1 - \frac{\gamma}{\beta + \gamma} e^{-\beta t}, \tag{11}$$

where N_∞ is the total number of water molecules per unit volume at saturation and κ is defined as:

$$\kappa = \frac{\pi^2 D_L}{4h^2}. \tag{12}$$

The total number of water molecules per unit volume at the pseudo-equilibrium state, N_{pe}, may be obtained as [6]:

$$\frac{N_{pe}}{N_\infty} = \frac{\beta}{\beta + \gamma}. \tag{13}$$

2.3. Fickian Model in Desorption

The desorption process was modeled using Fick's law as:

$$\begin{cases} \frac{\partial C(x,t)}{\partial t} = D_d \frac{\partial^2 C(x,t)}{\partial x^2} \\ C(x = \pm h,\ t) = C_r, \\ C(x, t \le 0) = C_\infty \end{cases} \tag{14}$$

where D_d and C_r are the diffusion coefficient of the desorption process and the minimum retained water concentration, respectively. The solution of this differential equation set for time t and spatial coordinate x is:

$$\frac{C(x,t) - C_r}{C_\infty - C_r} = \frac{4}{\pi} \sum_{n=0}^{\infty} \frac{(-1)^n}{2n+1} \exp\left(\frac{-D_d (2n+1)^2 \pi^2 t}{4h^2}\right) \cos\frac{(2n+1)\pi x}{2h}. \tag{15}$$

The fractional retained mass of water in the adhesive sample in percentage at time t, M_t^l, can be obtained by integrating Eq. (15) over the spatial variable:

$$\frac{M_t^l - M_r}{M_\infty - M_r} = \frac{8}{\pi^2} \sum_{n=0}^{\infty} \frac{1}{(2n+1)^2} \exp\left(\frac{-D_d (2n+1)^2 \pi^2 t}{4h^2}\right), \tag{16}$$

where M_r is the minimum fractional retained water.

3. EXPERIMENTAL PROCEDURE

Two different proprietary, commercial DGEBA-based heat-cured rubber-toughened structural epoxy adhesives were studied (Table 1). The recommended curing profiles were at least 30 min at 180°C, monitored using a thermocouple embedded in the adhesive layer.

TABLE 1 Mechanical and Physical Properties of Adhesives 1 and 2 as Supplied by the Manufacturers

Adhesive	Elastic modulus, E (Mpa)	Poisson's ratio, ν	Tensile strength, σ_y (Mpa)	Glass transition temp, T_g (°C)	Cured density (g/cm^3)
Adhesive 1	1.96	0.45	44.8	125	1.50
Adhesive 2	1.73	0.39	N/A	122	1.14

Adhesive wafers were cast between two aluminum plates coated with a polytetrafluroethylene release agent. The wafer thickness of 0.8 mm was controlled using spacing wires. After curing, the adhesive wafers were cut to approximately 40×40 mm ensuring that the diffusion process was essentially one-dimensional in the thickness direction (the edge surface area was less than 4% of the total). A sharp knife was used to prevent edge cracking. XPS indicated some traces of release agent (fluorine) on the wafer surfaces; however, the gravimetric results did not change when this was sanded off.

To remove any absorbed moisture, the wafers were kept in a vacuum oven containing anhydrous calcium sulphate at 40°C for approximately 7 days. Mass uptake measurements were made under different combinations of temperature and RH as given in Table 2 along with the saturated salt solutions used to generate the atmospheres [18,19]. Table 2 also gives the amount of water present per unit volume of atmosphere at each exposure condition [20]. Airtight plastic containers were used as conditioning chambers within temperature-controlled ovens, and the wafers were placed on a grating

TABLE 2 Different Exposure Conditions for Adhesives 1 and 2 and Saturated Salt Solutions Used to Achieve Different Levels of RH

		Temperature (°C)							
		20		40		50		60	
RH (%)	Salt solution	H_2O content (g/m^3)	Adh. studied	H_2O content (g/m^3)	Adh. studied	H_2O content (g/m^3)	Adh. studied	H_2O content (g/m^3)	Adh. studied
31	$MgCl_2$	5.5	N/A	16.2	1	26.2	N/A	41.0	N/A
43	K_2CO_3	7.4	1	21.7	1	35.2	N/A	55.1	1
75	NaCl	12.9	N/A	37.9	1	61.4	N/A	96.1	N/A
82	KCl	14.1	1	41.5	1 & 2	67.1	1	105.1	1 & 2
95	K_2SO_4	16.3	1 & 2	48.0	1 & 2	77.8	1	121.7	1 & 2

with point contacts. Absorption and desorption measurements were repeated on three wafers at each exposure condition. Desorption was carried out in a vacuum oven containing anhydrous calcium sulphate at 40°C for up to 3 months. Some of the samples were analysed in fresh, saturated, and dried states using XPS to investigate changes in the composition due to water ingress.

4. RESULTS AND DISCUSSION

4.1. Moisture Absorption

Both the new sequential dual Fickian (SDF) and the Langmuir models were used to characterize moisture diffusion into Adhesives 1 and 2. It was assumed that the diffusion coefficients D_1 and D_2 in the SDF model and D_L for the Langmuir model were independent of time. D_1 was determined by assuming a linear relationship between normalized mass uptake, $M_t/M_{1\infty}$, and $t^{1/2}$ during the initial stages of absorption. This linear relationship was approximated by [21]:

$$\frac{M_t}{M_{1\infty}} = \frac{2}{h}\left(\frac{D_1 t}{\pi}\right)^{1/2}. \tag{17}$$

It was assumed that the samples were fully saturated during the absorption period and the total saturated fractional mass uptake, M_∞ ($=M_{1\infty}+M_{2\infty}$), was determined from the gravimetric data. The other three parameters of SDF model ($M_{1\infty}$, t_d and D_2) were determined by curve fitting. A nonlinear, least-squares optimization approach was developed using MATLAB® programming to find the best fit of Eq. (6) to the experimental data points. In the Langmuir model, the diffusion coefficient, D_L, was assumed to be equivalent to D_1 in the SDF model. The probabilities β and γ were found by a least-squares fitting of the analytical model to the experimental data points. Following the formulation and procedure given in [8,9], the parallel dual Fickian (PDF) model was also fitted to the experimental results using a least-squares optimization approach in MATLAB® to compare with the SDF and Langmuir models.

4.1.1. Fractional Mass Uptake Profiles of Adhesive 1

Figures 2–4 show the measured fractional mass uptake, M_t, and the fitted SDF, Langmuir, and PDF models *versus* the square root of time ($t^{1/2}$) for Adhesive System 1 at different RH values for three temperatures. After the initial linear Fickian diffusion and the onset of a plateau, a second mass increase was observed in most of the

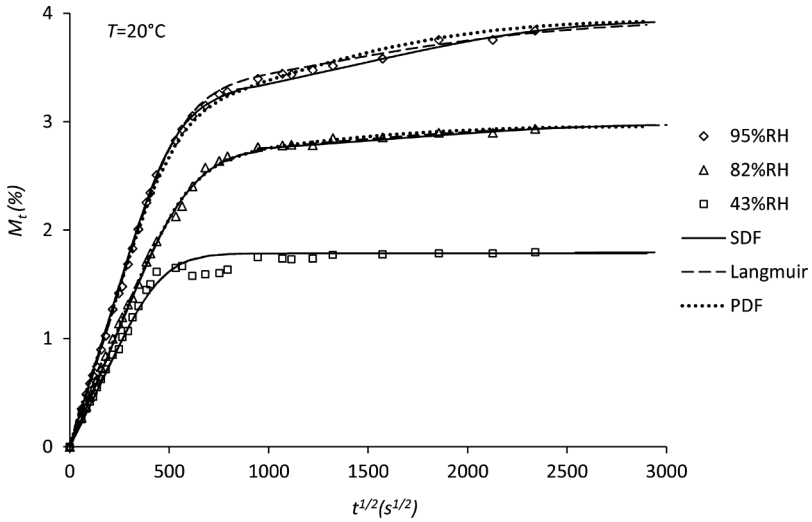

FIGURE 2 Measured fractional mass uptake *versus* square root of time and the least-squares fits based on the SDF, Langmuir, and PDF models at three RH levels for Adhesive 1 at 20°C. Each data point is an average of three repetitions.

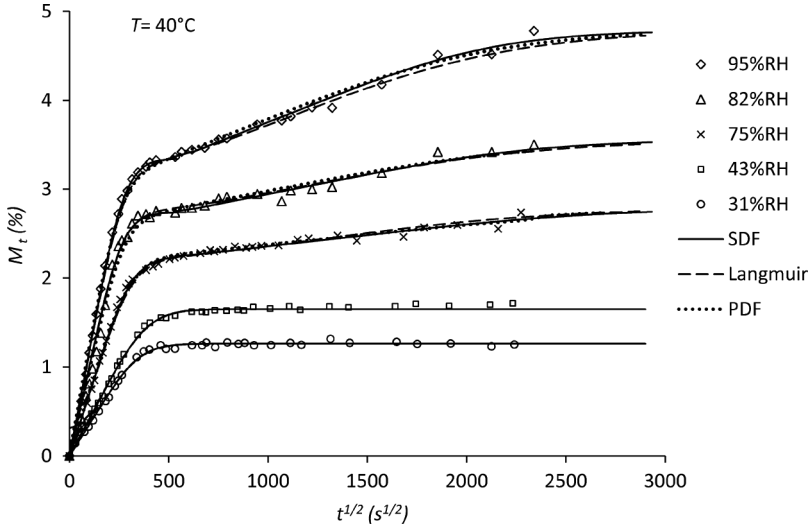

FIGURE 3 Measured fractional mass uptake *versus* square root of time and the least-squares fits based on the SDF, Langmuir, and PDF models at five RH levels for Adhesive 1 at 40°C. Each data point is an average of three repetitions.

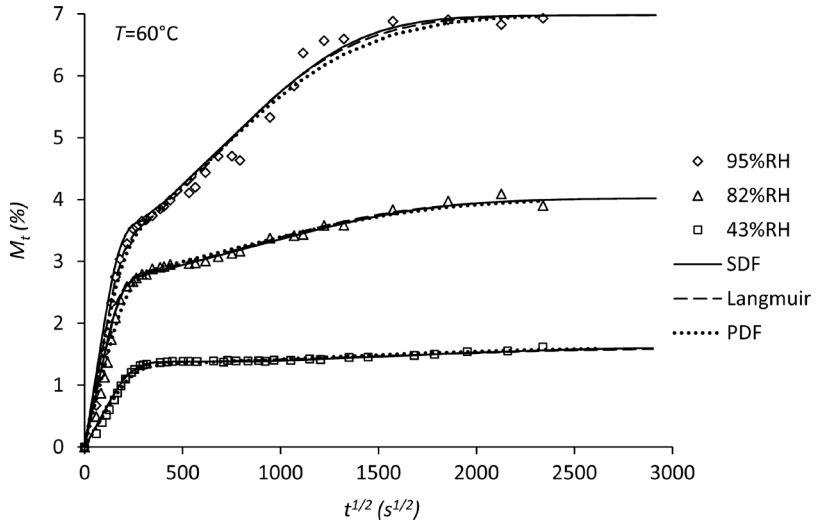

FIGURE 4 Measured fractional mass uptake *versus* square root of time and the least-squares fits based on the SDF, Langmuir, and PDF models at three RH levels for Adhesive 1 at 60°C. Each data point is an average of three repetitions.

exposure conditions. The single-stage Fickian model, thus, overestimated the experimental results, especially at high temperatures and RH, and at intermediate times.

Tables 3 and 4 list the parameters of the SDF and Langmuir models, respectively, for Adhesive 1 under the different exposure conditions. At the lower temperatures and RH (40°C-43% RH, 40°C-31% RH, 20°C-43% RH), the second diffusion mechanism disappeared and the fractional mass uptake profiles followed a simple Fickian diffusion behaviour ($D_2 = 0$, $t_d = \infty$, $M_{2\infty} = 0$). In these cases, the pseudo-equilibrium and final equilibrium states of the Langmuir model become coincident and there is no unique solution because any β with $\gamma = 0$ satisfies the model. Therefore, the Langmuir model was not used in these cases.

4.1.2. Fractional Mass Uptake Profiles of Adhesive 2

Figure 5 shows the experimental fractional mass uptake, M_t, *versus* square root of time ($t^{1/2}$) and the fitted SDF, Langmuir, and PDF models at 20, 40, and 60°C and 95% RH for Adhesive 2. The corresponding parameters for both models are given in Tables 5 and 6.

The SDF model was able to characterize the anomalous diffusion behaviour of Adhesives 1 and 2, showing a good agreement with the

TABLE 3 SDF Model Parameters Obtained by Curve Fitting the Experimental Gravimetric Results at Different Combinations of Temperature and RH for Adhesive 1

T (°C)	RH (%)	$D_1 = D_L \pm$ SD (10^{-14} m^2/s)	$D_2 \pm$ SD (10^{-14} m^2/s)	$M_{1\infty} \pm$ SD (%) (SDF)	$M_\infty = N_\infty \pm$ SD (%)	$t_d^{1/2}$ ($s^{1/2}$)	$M_{1\infty}$ (%) (PDF)
20	95	36 ± 6	3.9 ± 0.6	3.31 ± 0.05	3.94 ± 0.06	845	2.72
	82	33 ± 5	3.5 ± 0.5	2.77 ± 0.02	2.96 ± 0.02	941	2.25
	43	45 ± 6	0.0	1.78 ± 0.04	1.78 ± 0.04	∞	1.78
40	95	134 ± 17	3.8 ± 0.7	3.36 ± 0.09	4.78 ± 0.15	536	2.80
	82	142 ± 6	3.3 ± 0.4	2.71 ± 0.04	3.55 ± 0.06	524	2.34
	75	159 ± 25	3.6 ± 0.6	2.21 ± 0.05	2.79 ± 0.06	521	1.97
	43	113 ± 11	0.0	1.65 ± 0.04	1.65 ± 0.04	∞	1.65
	31	139 ± 19	0.0	1.26 ± 0.04	1.26 ± 0.04	∞	1.26
50	95	207 ± 9	4.5 ± 0.7	3.59 ± 0.08	6.67 ± 0.17	427	3.11
	82	222 ± 12	3.6 ± 0.4	2.71 ± 0.02	3.69 ± 0.04	416	2.28
60	95	314 ± 25	8.6 ± 0.9	3.73 ± 0.11	6.98 ± 0.18	329	2.59
	82	294 ± 28	4.9 ± 0.7	2.75 ± 0.05	4.02 ± 0.08	308	2.39
	43	271 ± 24	4.3 ± 0.8	1.38 ± 0.03	1.62 ± 0.04	924	2.72

$M_{1\infty}$ values obtained from PDF model are also given. Each data point is given as an average of three values obtained from the repetitions. SD shows the standard deviation.

experimental results, the Langmuir model, and the PDF model. Using the Langmuir model provides a means to estimate the relative amounts of bound and free water molecules in the adhesive. However, the probabilities β and γ have no physical significance in the diffusion process and also must be adjusted for any new exposure condition

TABLE 4 Langmuir Model Parameters Obtained by Curve Fitting to the Experimental Gravimetric Results at Different Combinations of Temperature and RH for Adhesive System 1

T (°C)	RH (%)	$\beta \pm$ SD (10^{-7}/s)	$\gamma \pm$ SD (10^{-7}/s)	N_{pe} (%)
20	95	3.23 ± 0.19	0.68 ± 0.03	3.23 ± 0.08
	82	3.46 ± 0.14	0.43 ± 0.02	2.63 ± 0.06
40	95	4.07 ± 0.26	1.94 ± 0.12	3.20 ± 0.09
	82	3.66 ± 0.18	1.23 ± 0.05	2.66 ± 0.07
	75	3.43 ± 0.16	0.88 ± 0.04	2.18 ± 0.04
50	95	4.97 ± 0.22	5.31 ± 0.28	3.20 ± 0.08
	82	4.78 ± 0.15	1.75 ± 0.06	2.69 ± 0.06
60	95	10.9 ± 0.81	12.86 ± 0.73	3.21 ± 0.11
	82	6.88 ± 0.43	3.22 ± 0.22	2.75 ± 0.05
	43	2.52 ± 0.14	0.53 ± 0.04	1.36 ± 0.04

Each data point is given as an average of three values obtained from the repetitions. SD shows the standard deviation.

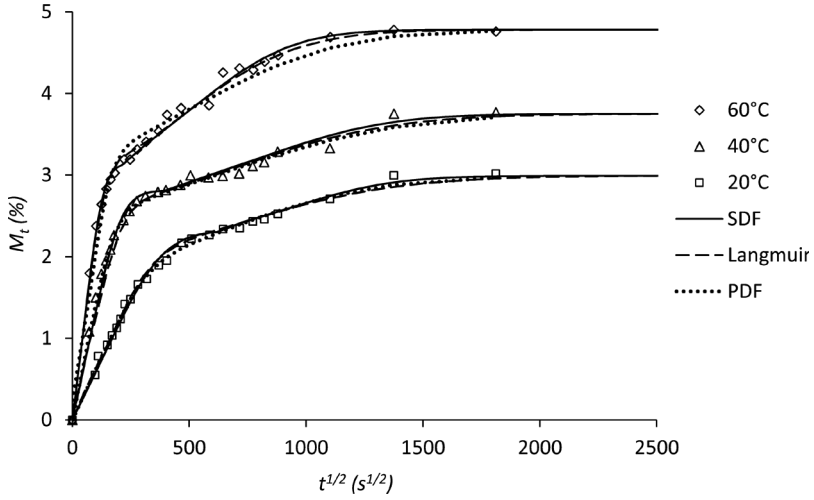

FIGURE 5 Measured fractional mass uptake *versus* square root of time and the least-squares fits based on the SDF, Langmuir, and PDF models at 95% RH and three different temperatures for Adhesive 2. Each data point is an average of three repetitions.

(Section 4.1.6). The SDF model divides the diffusion process into two separate stages governed by Fick's law, which has a physical significance. The predictions of the SDF and PDF models were very similar, deviating the most at high RH and intermediate exposure times close to t_d. The $M_{1\infty}$ values obtained from the SDF model agree well with the total number of water molecules per unit volume in the pseudo-equilibrium state (N_{pe}) of the Langmuir model (average

TABLE 5 SDF Model Parameters Obtained by Curve Fitting to the Experimental Gravimetric Results at Different Combinations of Temperature and RH for Adhesive 2

T (°C)	RH (%)	$D_1 = D_L \pm$ SD (10^{-14} m^2/s)	$D_2 \pm$ SD (10^{-14} m^2/s)	$M_{1\infty} \pm$ SD (%) (SDF)	$M_\infty = N_\infty \pm$ SD (%)	$t_d^{1/2}$ ($s^{1/2}$)	$M_{1\infty}$ (%) (PDF)
20	95	26 ± 4	6.8 ± 1.2	2.31 ± 0.04	2.99 ± 0.06	631	1.87
40	95	87 ± 11	4.1 ± 0.8	2.83 ± 0.06	3.75 ± 0.09	386	2.41
	82	104 ± 13	9.8 ± 1.5	2.14 ± 0.06	2.27 ± 0.07	497	1.78
60	95	248 ± 29	8.1 ± 1.5	3.16 ± 0.09	4.78 ± 0.12	219	2.59
	82	208 ± 24	9.6 ± 1.3	2.38 ± 0.03	2.8 ± 0.04	273	1.99

$M_{1\infty}$ values obtained from PDF model are also given. Each data point is an average of three values obtained from the repetitions. SD shows the standard deviation.

TABLE 6 Langmuir Model Parameters Obtained by Curve Fitting to the Experimental Gravimetric Results at Different Combinations of Temperature and RH for Adhesive 2

T (°C)	RH (%)	$\beta \pm$ SD (10^{-7}/s)	$\gamma \pm$ SD (10^{-7}/s)	$N_{pe} \pm$ SD (%)
20	95	10.88 ± 0.73	5.8 ± 0.34	2.06 ± 0.04
40	95	10.64 ± 0.84	4.7 ± 0.29	2.58 ± 0.08
	82	12.5 ± 0.87	1.1 ± 0.06	2.08 ± 0.07
60	95	22.3 ± 1.38	12.9 ± 0.69	3.10 ± 0.10
	82	24.2 ± 1.82	0.5 ± 0.03	2.32 ± 0.06

Each data point is an average of three values obtained from the repetitions. SD shows the standard deviation.

difference of 4%; see Section 4.1.5). This agreement adds physical significance to $M_{1\infty}$ in the SDF model. The $M_{1\infty}$ values obtained from the PDF model were always lower than the corresponding N_{pe} values with an average difference of 15%. As will be discussed in Section 4.1.4, it is reasonable to assume that some of the water diffusion mechanisms occur after a delay time (*i.e.,* t_d), leading to the second stage of water uptake; therefore, the SDF model is believed to represent a more realistic representation of water diffusion in the present adhesives.

Furthermore, it has been reported that in some cases the pseudo-equilibrium state ($M_{1\infty}$ occurring after t_d) for water absorption by DGEBA-based epoxies can be much longer than was found with the present adhesives [8,22]. Since the PDF model assumes that both of the diffusion mechanisms start from the beginning of the absorption process, the predicted mass uptake always increases with time and it is difficult to model such absorption behavior accurately. To deal with this limitation, Mubashar *et al.* [8] used a "delayed SDF" model by adding a power function to the SDF formulation. This delayed SDF model, however, adds three more constants and so increases the degrees of freedom of the problem, making it more difficult to develop the ability to predict how the model parameters vary with temperature and RH. As with the original PDF model, there is no physical significance to the added power function. On the other hand, by assuming two sequential water uptake stages, the SDF model provides a more general water absorption model that relates to the physical significance of Fick's law and the Langmuir model.

In general, Adhesive 2 appeared to be more resistant to water ingress than Adhsive 1, and all five SDF parameters (D_1, D_2, $C_{1\infty}$, $C_{2\infty}$, t_d) for Adhesive 2 were always less than those for Adhesive 1 at the same exposure condition. The D_1 and M_∞ values of Adhesive 2

were approximately 28 and 26% lower than those of Adhesive 1, respectively.

In order for the SDF and Langmuir models to be predictive beyond the ambient conditions used in the experiments, it is necessary to identify the dependence of the model parameters on temperature and RH. This is discussed in the following subsections. It is noted that the present experiments did not investigate the possibility that the adhesive thickness influences the diffusion properties as reported in [9]. However, such changes were reported to be relatively small, being of the same order as the experimental scatter (*e.g.*, Table 4). Moreover, Ref. [9]. did not provide an explanation for the observed dependency on adhesive thickness; therefore, the generality of this phenomenon remains unknown.

4.1.3. The Effect of Temperature and RH on the Diffusion Coefficients

Analysis of variance showed that D_1 for Adhesive 1 was independent of RH at all temperatures (95% confidence). Similarly, in the case of Adhesive 2, a *t*-test showed that the average values of D_1 were independent of RH at all temperatures. The second diffusion coefficient, D_2, was always appreciably less than D_1 for both adhesives (Tables 3 and 5). Excluding the inexplicably high D_2 value at the 60°C-95% RH condition for Adhesive 1, and unexpectedly low value at 40°C-95% RH condition for Adhesive 2, analysis of variance revealed that D_2 could be assumed independent of temperature and RH (95% confidence) for both adhesives.

The Arrhenius rate equation was used to investigate the effect of temperature on D_1:

$$D_1 = D_0 \exp\left(-\frac{Q}{RT}\right), \tag{18}$$

where D_0 and Q are the diffusion constant and activation energy, respectively. R is the universal gas constant (0.00198 kcal/K.mol) and T is absolute temperature (K). Figure 6 shows D_1 *versus* inverse temperature, $1/T$, on a logarithmic scale for both adhesives. At a given temperature, D_1 was taken as the average obtained from the different RH conditions, since it was independent of RH as described above. Least squares regression showed that the D_1 variation with $\exp(1/T)$ was sufficiently linear in both adhesives during the first diffusion process to be modeled using Eq. (18). The calculated activation energy of the first diffusion process was essentially the same for Adhesives 1 and 2, *i.e.*, 10.2 and 10.6 kcal/mol, respectively.

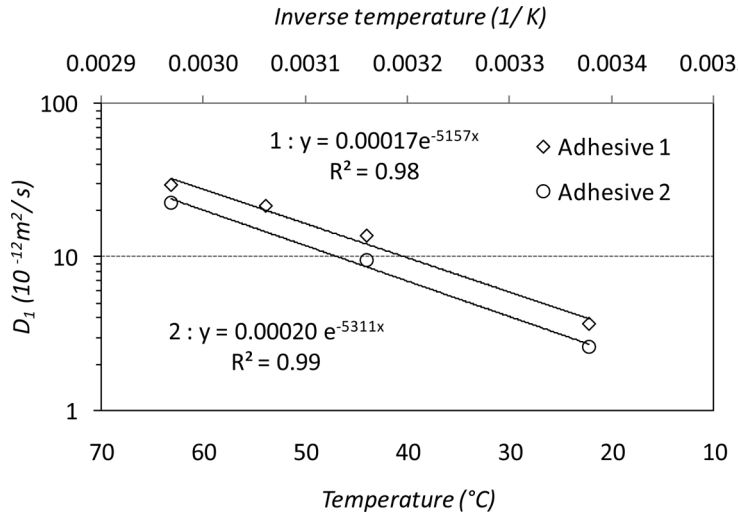

FIGURE 6 Variation of first diffusion coefficient, D_1, with temperature for Adhesives 1 and 2. At each temperature, D_1 was taken as the average obtained from different RH conditions. Linear fit to the Arrhenius equation [Eq. (18)] with the slope equal to $-Q/R$.

By way of comparison, Atkins reported that the energy required for breaking the hydrogen bonds present in liquid water (O-H $\cdots$ O) ranges from 5–20 kcal/mol [23]. The activation energy of the main-chain bonding of the epoxy network was reported to be 60–100 kcal/mol, and that of physical bonding (Van der Waals and/or dipole-dipole) is 0.5–2 kcal/mol [14]. Zhou and Lucas also reported the activation energy of water diffusion in a DGEBA-based epoxy to be 9.3 kcal/mol and attributed it to hydrogen bonding [14]. Therefore, the average activation energy of approximately 10 kcal/mol for both adhesives falls within the range reported for that of water diffusion in epoxy as well as the energy of hydrogen bonding given in the literature.

Popineau *et al.* [6] studied the kinetics of absorbed water in epoxy and concluded that the first diffusion mechanism corresponds to the diffusion of water molecules having strong interactions with the epoxy, while the water molecules absorbed during the second diffusion mechanism are relatively mobile. The second diffusion mechanism can then be related to a physical phenomenon such as clustering, in which the water molecules fill the free volume of the epoxy [9]. The water molecules within a cluster have no strong connections with the epoxy backbone and are essentially free.

4.1.4. The Effect of Temperature and RH on the Saturated Fractional Mass Uptakes

As seen in Fig. 7, $M_{1\infty}$ increased significantly with RH, but it remained almost independent of temperature. This indicates that temperature affected only the rate of the first diffusion mechanism and not its saturation concentration value.

Figure 7 also shows that $M_{2\infty}$ increased with both temperature and RH, although saturation in the second stage was not reached over the durations of the present experiments at the lowest temperature and RH exposure conditions (20°C-43% RH, 40°C-43% RH).

The dependence of $M_{2\infty}$ on RH and temperature can be explained in terms of the clustering of water molecules which is hypothesized to have occurred during the second uptake. One of the main factors that can increase the potential sites for the clustering is volumetric swelling of the adhesive due to water absorption, which will increase with both RH and temperature. The swelling strain is negligible during the initial stage of exposure but starts to increase (up to 10%) from medium exposure times [9,24,25]. It is then reasonable to assume that the volumetric expansion caused by the diffusion of water into the adhesive does not act immediately, which supports the assumption of a transition time, t_d. The expansion causes the enlargement of the potential clustering sites within the adhesive and water molecules can then diffuse to fill these new voids.

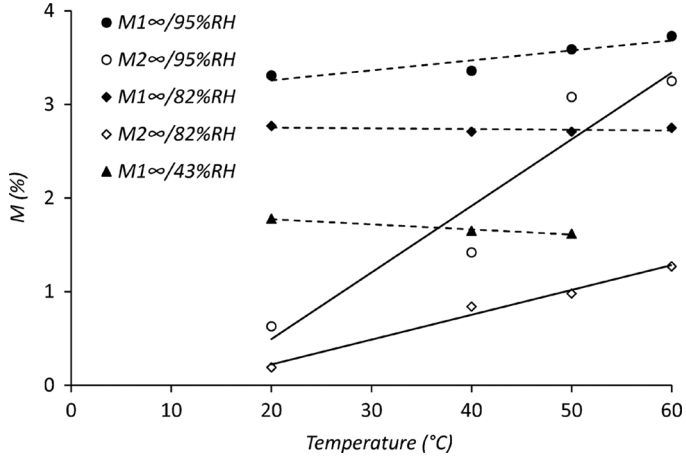

FIGURE 7 Variation of the first and second saturated fractional mass uptake values, $M_{1\infty}$ and $M_{2\infty}$, with temperature at 95, 82, and 43% RH for Adhesive 1. The lines are least squares fits. Each data point is an average of three repetitions.

An increase in the free volume for clustering and, hence, $M_{2\infty}$, can also occur because of thermal expansion and osmotic pressure within water clusters, both of which will depend on temperature and RH [26]. Osmotic pressure can be created by the diffusion of soluble components such as fillers into water clusters [27], thereby expanding the epoxy network. The water diffusion mechanism activated by osmotic pressure can then be assumed to start after the formation of water clusters at a later time (t_d) instead of the beginning of the diffusion ($t = 0$). The osmotic expansion and its contribution to $M_{2\infty}$ will be proportional to the amount of absorbed water which is a function of temperature and RH. The absence of second stage within the period of the experiments at the lowest temperature and RH (20°C-43% RH, 40°C-43% RH) can be attributed to the relatively slow rate of volumetric expansion.

4.1.5. The Effect of Temperature and RH on the Transition Time

As seen in Table 3, t_d remained mostly unchanged with RH at different temperatures for Adhesive 1, except for the 60°C-43% RH condition in which the transition time appeared to be unexpectedly long. It varied slightly with RH for the conditions studied with Adhesive 2 (Table 5). Noting that the first diffusion mechanism was shown to be a chemical interaction (hydrogen bonding) which followed the Arrhenius rate equation, it is reasonable to assume that the time required for the first process to be completed (t_d) depends on the rate of the process (D_1). If it is hypothesized that t_d has an inverse linear relationship with D_1 as:

$$t_d = KD_1^{-1}, \tag{19}$$

where K is a constant, then substituting D_1 from Eq. (18) into Eq. (19) results in

$$t_d = t_{d0} \exp\left(\frac{Q}{RT}\right), \tag{20}$$

where $t_{d0} = KD_0$ is a transition time constant. To examine this hypothesis, the activation energy of the first diffusion mechanism, Q, was calculated using Eq. (20) and the measured t_d. Figure 8 shows the variation of t_d with inverse temperature on a logarithmic scale at 95% RH for both adhesives. Very similar results were observed at 82% RH for Adhesive 1. A very good linear least squares fit between t_d and $\exp(1/T)$ suggested that Eq. (19) was a valid assumption and using these fits, Q for Adhesives 1 and 2 was found to be 9.7 and 10.2 kcal/mol, respectively. Using the results at 82% RH, Q for

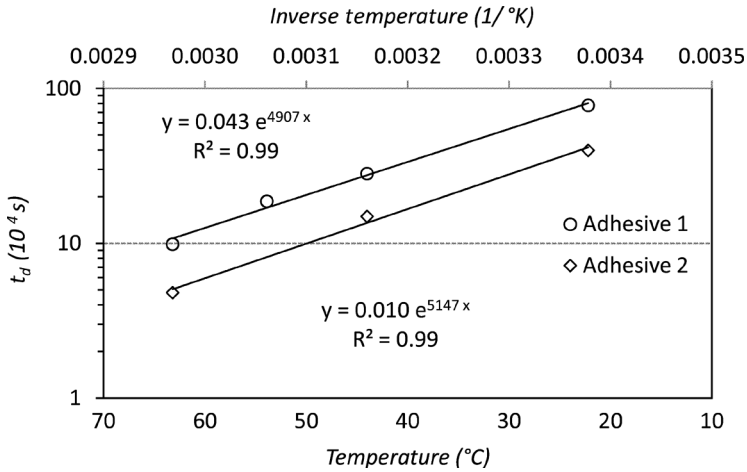

FIGURE 8 Variation of the transition time with temperature at 95% RH for both adhesives. Each data point is an average of three values obtained from the repetitions. The lines show least squares regressions between t_d and $\exp(1/T)$ and the slopes of the lines give the values of Q/R.

Adhesive 1 was calculated to be 10.1 kcal/mol. These values compare well with those calculated for D_1 using the data of Fig. 6, differing by only 5 and 3%, respectively.

Furthermore, the fractional mass uptake at t_d, $M_{1\infty}$, agrees well with the pseudo-equilibrium mass uptake, N_{pe}, of the Langmuir model at any exposure condition with an average difference of about only 4% (Fig. 9). Therefore, t_d of the SDF model corresponds to the pseudo-equilibrium state of the Langmuir model. These results lend confidence that t_d as the time of saturation for the first diffusion mechanism was properly determined.

4.1.6. The Effect of Temperature and RH on the β and γ Probabilities of Langmuir Model

Figure 10 shows the variation of β and γ with inverse temperature on a logarithmic scale at 82% RH for Adhesive 1. The fairly linear fits indicate that both probabilities varied approximately exponentially with T and followed the Arrhenius rate equation at a particular RH. Similarly at 95% RH, both β and γ varied exponentially with T but with different rates. Figure 11 shows that β and γ also depended strongly on RH, especially at higher temperature. Hence, although the form of the Langmuir model fits absorption data well, it does so with adjustable parameters β and γ that are unknown functions of

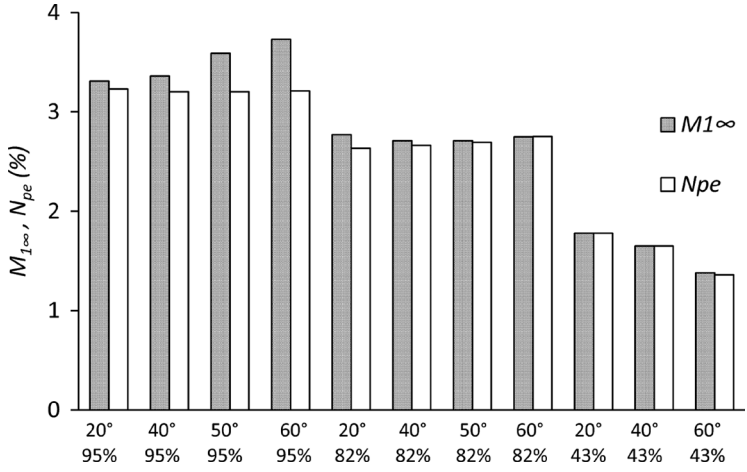

FIGURE 9 Comparison between the first saturated fractional mass uptake, $M_{1\infty}$, of the SDF model and the pseudo-equilibrium mass uptake, N_{pe}, of the Langmuir model at different combinations of temperature and RH. Each data point is an average of three values obtained from the repetitions.

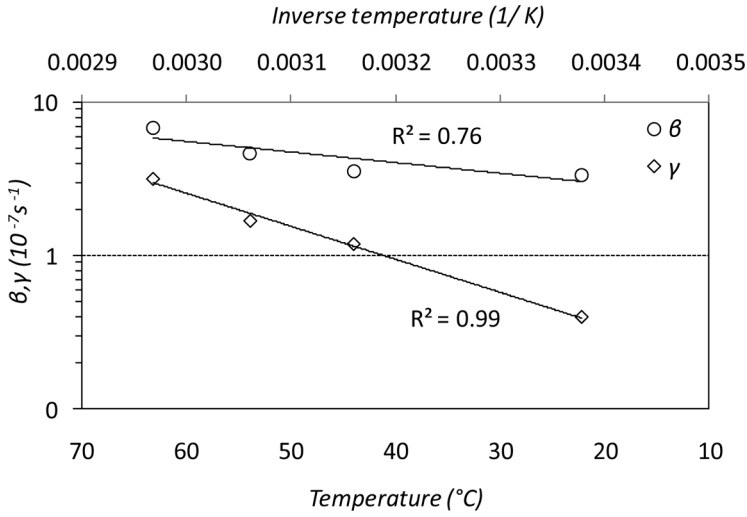

FIGURE 10 Variation of β and γ probabilities with temperature at 82% RH for Adhesive 1. Each data point is an average of three values obtained from the repetitions. The lines show least squares regressions between the probabilities and $\exp(1/T)$.

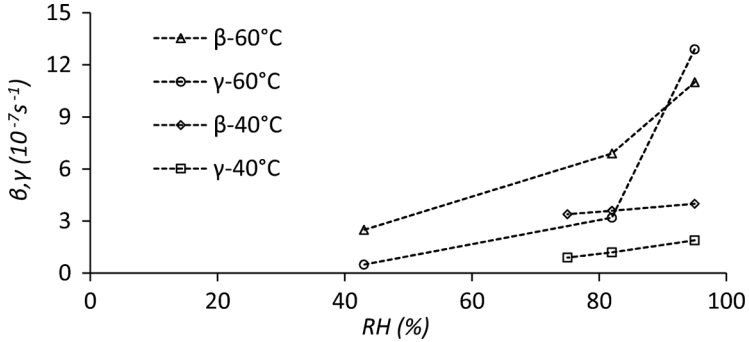

FIGURE 11 Variation of β and γ probabilities with RH at temperatures of 40 and 60°C for Adhesive 1. Each data point is an average of three values obtained from the repetitions. The lines are only to guide the trends.

both temperature and RH. This limits the use of the Langmuir model to environments where β and γ have been determined, and makes interpolation and extrapolation to different environments uncertain.

4.2. Moisture Desorption

After the absorption process, the samples were dried in a vacuum oven at 40°C to measure the desorption profiles. The mass of samples decreased uniformly with drying time to minimum fractional retained water, M_r (%), and remained unchanged, even after approximately 3 months. The simple Fickian model sufficiently characterized the desorption process in both adhesives in terms of the desorption diffusion coefficient, D_d, the saturated fractional mass uptake, M_∞, and the minimum fractional retained water, M_r. D_d was determined in the same manner as D_1 using Eq. (17) and normalized mass loss profiles.

4.2.1. Fractional Retained Mass Profiles of Adhesives 1 and 2

Figures 12–14 show the experimentally measured fractional retained mass, M_t^l, *versus* square root of time, $t^{1/2}$, and Fickian fits for the wafers of Adhesive 1 that had been exposed to different RH at 20, 40, and 60°C. Figure 15 shows the same results for Adhesive 2 with the exposure condition of 60°C-95% RH. No second slope was observed during desorption and the simple Fickian model adequately characterized the behaviour of both adhesives. The main difference between the fractional retained mass profiles of Adhesives 1 and 2 was the minimum fractional retained water, M_r—1.4 and 0.16%, respectively, for the same M_∞ of 4.8%. The M_r value for Adhesive 1 was approximately 30% of the corresponding M_∞.

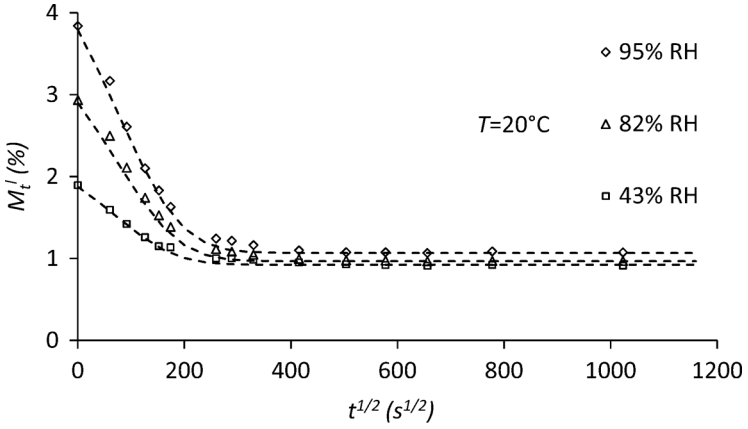

FIGURE 12 Fractional retained mass during drying *versus* square root of time, fitted with the simple Fickian model for Adhesive 1 initially saturated at 20°C and different RH. Each data point is an average of three repetitions.

As mentioned previously, Marsh *et al.* [15] and Moy and Karasz [16] concluded that a drying temperature above T_g was required to completely remove absorbed water from epoxy resin. Zhou and Lucas [14] observed some retained water in both DGEBA- and TGDDM-based epoxies after drying at temperatures up to 90°C, which was greater than T_g. They found that the amount of retained water eventually reached zero, but the activation energy required for high-temperature

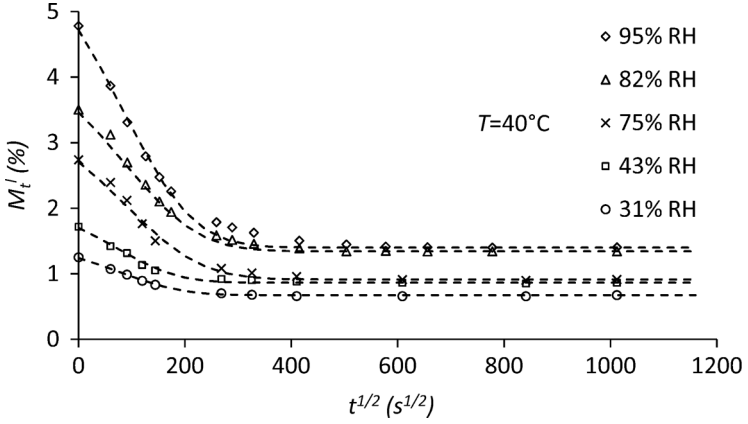

FIGURE 13 Fractional retained mass during drying *versus* square root of time, fitted with simple Fickian models for Adhesive 1 initially saturated at 40°C and different RH. Each data point is an average of three repetitions.

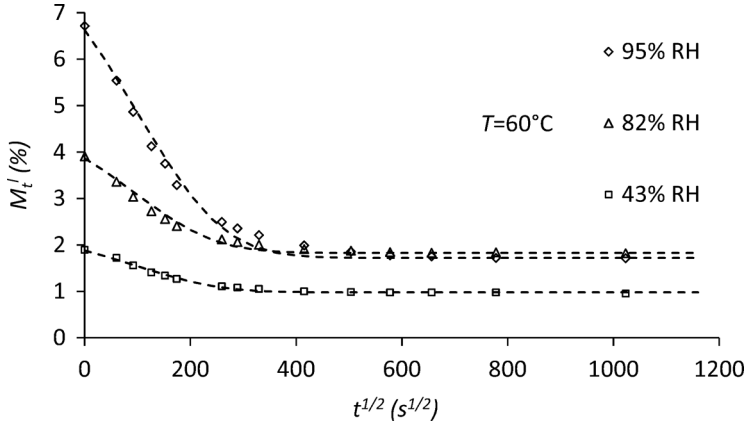

FIGURE 14 Fractional retained mass during drying *versus* square root of time and fitted simple Fickian models for Adhesive 1 initially saturated at 60°C and different RH. Each data point is an average of three repetitions.

desorption was higher than that of low-temperature desorption. They concluded that the water molecules retained after low-temperature desorption had multiple hydrogen bonds with the epoxy network.

4.2.1. The Effect of Temperature and RH on the Minimum Fractional Retained Water

Figures 16 and 17 show that M_r was proportional to the temperature and RH during the absorption process for Adhesive 1. At low

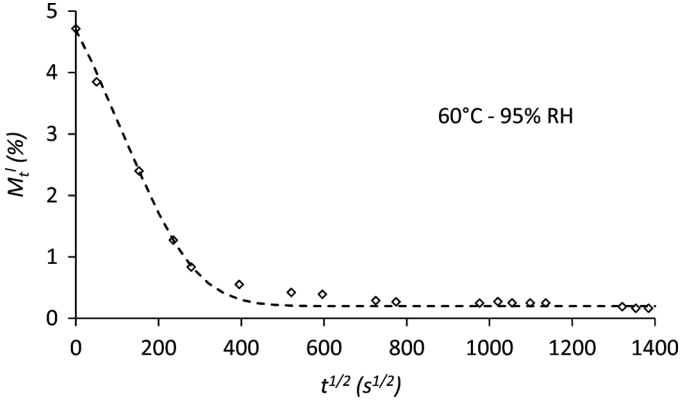

FIGURE 15 Fractional retained mass profile during drying *versus* square root of time and fitted simple Fickian model for Adhesive 2 initially saturated at 60°C-95% RH. Each data point is an average of three repetitions.

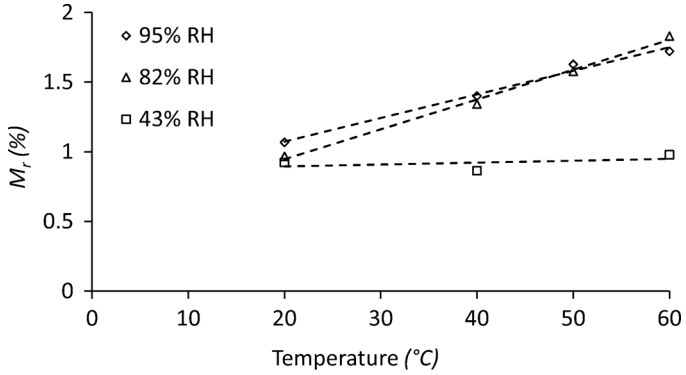

FIGURE 16 Variation of minimum fractional retained water, M_r, with the temperature of absorption condition at different RH levels for Adhesive 1. Each data point is an average of three repetitions. The linear least squares fits show the general trends.

temperature (20°C), M_r remained relatively unchanged with RH (Fig. 17). Similarly, at low RH (43%), M_r was largely independent of T. Figure 18 also shows that M_r increased linearly with the ambient water concentration during absorption, regardless of temperature.

Figure 19 depicts the variation of minimum fractional retained water during the desorption process, M_r, with the saturated fractional mass uptake, M_∞ ($M_{1\infty} + M_{2\infty} = M_\infty$), which was obtained at different combinations of temperature and RH. M_r increased linearly with M_∞,

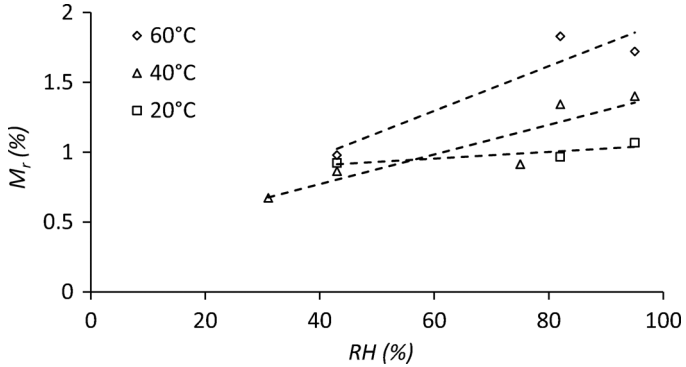

FIGURE 17 Variation of minimum fractional retained water, M_r, with the RH of the absorption condition at different temperatures for Adhesive 1. Each data point is an average of three repetitions. The linear least squares fits show the general trends.

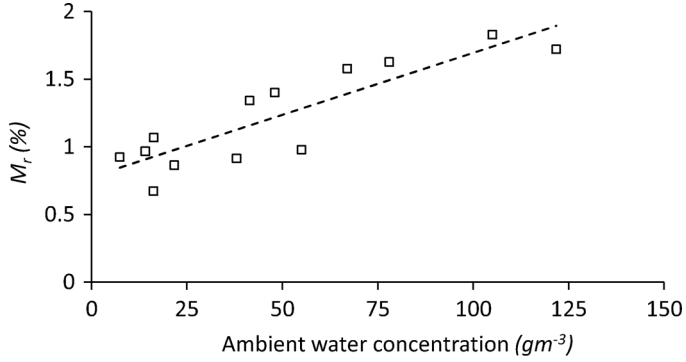

FIGURE 18 Variation of minimum fractional retained water, M_r, with the ambient water concentration achieved during different exposure conditions for Adhesive 1. Each data point is an average of three repetitions. The linear least squares fit shows the general trend.

independent of the original exposure condition. This finding may be useful in predicting the amount of retained water in the adhesive exposed to a varying environment.

4.3. XPS Analysis

The significant difference between M_r for these two adhesives was investigated using XPS. Table 7 shows the percentage of oxygen atoms associated with different chemical bonds (binding energies) for fresh (as-cured), saturated wet, and dried samples of Adhesives 1 and 2.

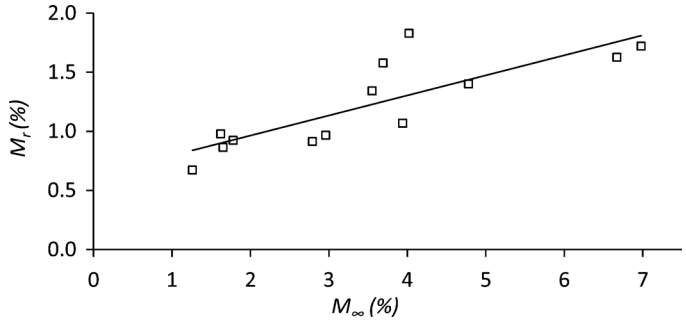

FIGURE 19 Variation of minimum fractional retained water during the desorption process with the saturated fractional mass uptake, M_∞, for Adhesive 1. Each data point is an average of three repetitions. The linear least squares fit shows the general trend.

TABLE 7 Percentage of Oxygen Atoms Associated with Different Chemical Bonds with Their Binding Energy for Fresh, Saturated Wet, and Dried Samples of Adhesives 1 and 2

	O1s		O1sA		O1sB	
Exposure condition: 60°C-95% RH	Atomic %	Binding energy (eV)	Atomic %	Binding energy (eV)	Atomic %	Binding energy (eV)
Adhesive 1						
Fresh ($M_t = 0$)	84	532.7	12	534.0	4	531.0
Wet ($M_t = M_\infty = 6.98\%$)	67	532.6	15	533.6	18	531.5
Dry ($M_t = M_r = 1.82\%$)	76	532.7	13	533.7	10	531.4
Adhesive 2						
Fresh ($M_t = 0$)	77	532.9	23	533.8	0	N/A
Wet ($M_t = M_\infty = 4.78\%$)	62	532.8	15	533.8	23	531.6
Dry ($M_t = M_r = 0.20\%$)	76	532.8	24	533.7	0	N/A

Each data point is an average of three repetitions.

The O1sB peak corresponded to a bond associated with water molecules since it was present in the wet samples of both adhesives, but not in the fresh and dried samples of Adhesive 2, nor was it significant in the fresh Adhesive 1. As seen in Table 7, the atomic percentage of O1sB was 10% in dried samples of Adhesive 1 which qualitatively supports the gravimetric results, indicating that a considerable amount of absorbed water in Adhesive 1 could not be removed during the drying process at 40°C.

5. CONCLUSIONS

The water absorption and desorption of two different rubber-toughened epoxy adhesives were characterized using gravimetric measurements. A newly developed sequential dual Fickian (SDF) model was developed to fit the fractional mass uptake profiles and agreed well with the Langmuir diffusion model. The diffusion mechanism in the first stage appeared to be influenced by hydrogen bonding while the diffusion mechanism in the second stage was primarily physical in nature. The diffusion coefficients in both stages were found to be largely independent of RH, while the saturated fractional mass uptake values increased with RH. The diffusion coefficient of the first stage and the saturated fractional mass uptake of the second stage were both functions of temperature. These functional dependencies were described, making the SDF model predictive over the ranges of temperature and RH that were investigated.

The desorption during drying in both adhesives was described well by Fick's law. Both gravimetric results and XPS revealed that there was a significant difference between the amounts of minimum fractional retained water in the two adhesives after drying. The relatively large amount of retained water in Adhesive 1 was attributed to multiple hydrogen bonds between the water molecules and the epoxy or other constituents such as the rubber toughener particles or the filler. In a separate test program, it was found that these differences in water absorption-desorption corresponded to marked differences in the degradation of fracture toughness in hot-wet aging environments (to appear in a future publication).

The SDF model can be used to predict the water concentration distribution in adhesive joints exposed to environments of changing temperature and RH under the assumption of negligible interface diffusion.

ACKNOWLEDGMENTS

The work was supported by General Motors Canada Ltd., the Natural Sciences and Engineering Research Council of Canada, and the Ontario Centres of Excellence.

REFERENCES

[1] LaPlante, G., Ouriadov, A. V., Lee-Sullivan, P., and Balcom, B. J., *J. Applied Polymer Science* **109**, 1350–1359 (2008).
[2] Fernandez-Garcia, M. and Chiang, M. Y. M., *J. Applied Polymer Science* **84**, 1581–1591 (2002).
[3] Musto, P., Ragosta, G., and Mascia, L., *Chem. Mater.* **12**, 1331–1341 (2000).
[4] Weir, M. D., Bastide, C., and Sung, C. S. P., *Macromolecules* **34**, 4923–4926 (2001).
[5] Masaro, L. and Zhu, X. X., *Prog. Polym. Sci.* **24**, 731–775 (1999).
[6] Popineau, S., Rondeau-Mouro, C., Sulpice-Gaillet, C., and Shanahan, M. E. R., *J. Polymer* **46**, 10733–10740 (2005).
[7] Roy, S., Xu, W. X., Park, S. J., and Liechti, K. M., *J. Applied Mechanics* **67**, 391–396 (2000).
[8] Mubashar, A., Ashcroft, I. A., Critchlow, G. W., and Crocombe, A. D., *Int. J. Adhesion Adhesives* **29**, 751–760 (2009).
[9] Loh, W. K., Crocombe, A. D., Abdel Wahab, M. M., and Ashcroft, I. A., *Int. J. Adhesion Adhesives* **25**, 1–12 (2005).
[10] Maggana, C. and Pissis, P. J., *Polym. Sci. Part B: Polym. Phys.* **37**, 1165–1182 (1999).
[11] Feng, J., Berger, K. R., and Douglas, E. P., *J. Mater. Sci.* **39**, 3413–3423 (2004).
[12] Carter, H. G. and Kibler, K. G., *J. Compos. Mater.* **12**, 118–131 (1978).
[13] Lin, Y. C., *J. Polymer Research* **13**, 369–374 (2006).
[14] Zhou, J. and Lucas, J. P., *J. Polymer* **40**, 5505–5512 (1999).
[15] Marsh, L. L., Lasky, R., Seraphim, D. P., and Springer, G. S., Moisture solubility and diffusion in epoxy and epoxy-glass composites in *Environmental Effects on*

Composite Materials, G. S. Springer (Ed.) (Technomic Publishing Co., Westport, 1988), p. 51.
[16] Moy, P. and Karasz, F. E., *Polym. Eng. Sci.* **20**, 315–319 (1980).
[17] Loh, W. K., Crocombe, A. D., Abdel Wahab, M. M., and Ashcroft, I. A., *J. Adhes.* **79**, 1135–1160 (2003).
[18] Loh, W. K., Crocombe, A. D., Abdel Wahab, M. M., and Ashcroft, I. A., *Eng. Frac. Mech.* **69**, 2113–2128 (2002).
[19] Greenspan, L., *J. Research National Bureau Standards A: Physics and Chemistry* **81**, 89–96 (1977).
[20] ASHRAE Handbook – *Fundamentals*, (American Society of Heating, Refrigerating and Air-Conditioning Engineers, Inc., 2009), I-P Edition, pp. 1.1–1.20.
[21] Wylde, J. W. and Spelt, J. K., *Int. J. Adhes. Adhes.* **18**, 237–246 (1998).
[22] De Neve, B. and Shanahan, M. E. R., *Int. J. Adhes. Adhes.* **12**, 191–196 (1992).
[23] Atkins, P. W., *Quanta*, (Oxford University Press, New York, 1990), 2nd ed., p. 68.
[24] El-Sa'ad, L., Darby, M. I., and Yates, B., *J. Mater. Sci.* **24**, 1653–1659 (1989).
[25] Chang, T., Lai, Y. H., Shephard, N. E., Sproat, E. A., and Dillard, D. A., *J. Adhes.* **60**, 153–162 (1997).
[26] Ivanova, K. I., Pethrick, R. A., and Affrossman, S., *J. Appl. Polym. Sci.* **82**, 3468–3476 (2001).
[27] Tu, Y. and Spelt, J. K., *J. Adhes.* **72**, 359–372 (2000).